On Endmember Detection in Hyperespectral Images with Morphological Associative Memories

Manuel Graña[1], Bogdan Raducanu[1], Peter Sussner[2], and Gerhard Ritter[3]

[1] Dept. CCIA, Universidad Pais Vasco, Spain,
`ccpgrrom@si.ehu.es`,
[2] Institute of Mathematics, Statistics and Scientific Computing, State University of Campinas, Brazil
[3] Center for Computer Vision and Visualization, University of Florida, USA.

Abstract. Morphological Associative Memories (MAM) are a construct similar to Hopfield Associative Memories defined on the $(R, +, \vee, \wedge)$ algebraic system. The MAM posses excelent recall properties for undistorted patterns. However they suffer from the sensitivity to specific noise models, that can be characterized as erosive and dilatative noise. We find that this sensitivity may be made of use in the task of Endmember determination for the Spectral Unmixing of Hyperespectral Images.

1 Introduction

Passive remote sensing evolution has produced measurement instruments with ever growing spectral bread and resolution. Multispectral sensing allows the classification of pixels, however the recognition that pixels of interest are frequently a combination of material has introduced the need to quantitatively decompose the pixel spectrum into their constituent material spectra. Hyperespectral sensor measurements in hundreds of spectral bands allow to perform such "spectral unmixing" [9]. The reasons for the mixture of several spectra in a sigle pixels are (1) the spatial resolution of the sensor implies that different land covers are included in the area whose radiance measurement results in an image pixel, and (2) distinct materials are intimately mixed (e.g.: a beach). The second situation is independent of the sensor spatial resolution and produces non-linear mixtures, which are difficult to analyze. The first situation produces mixtures which, often, can be adequately modelled by a linear mixing model. In this paper we assume that the linear model is correct, and we present an approach to the detection of endmembers for spectral unmixing in hyperespectral image processing through the application of Morphological Associative Memories.

Research efforts trying to introduce elements of mathematical morphology in the domain of the Artificial Neural Networks involve a small community but are sustained in time. In short definition Morphological Neural Networks are those that involve somehow the maximum and/or minimum (supremum and infimum) operators. Some fuzzy approaches are included in this definition. The kind of

Morphological Neural Networks range from patter classifiers [2], [12], [20], [28], target detection [5], [6], [14], [27], to associative memories for image restoration [16], [17], [18].

The basis for the learning algorithms is the computation of the gradient of functions that involve max/min operators [13],[27], [28], [29]. An antecedent for these works is the adaptive construction of morphological filters [1], [21]. Some authors [12], [13] propose the composition of the network with a mixture of morphological and linear operators in the nodes. The Morphological Associative Memories (MAM) [16], [17], [18] are the morphological couterpart of the Correlation Associative Memories (CAM) [10] and the well known Hopfield Associative Memories [7]. Like the CAM, MAM are constructed as correlation matrices but with the substitution of the conventional matrix product by a Min or Max matrix product from Image Algebra [19]. Dual constructions can be made using the dual Min and Max operators. We propose a procedure that involves the application of MAM to detect new patterns, but the training proceeds on line adding the patterns to the already identified patterns,

The structure of the paper is as follows: In section 2 we review the definition of the linear mixing model. Section 3 provides a review of basic results of MAM's. Section 4 gives our algorithm of endmember selection for remote sensing hyperespectral images. Section 5 presents some experimental results of the proposed algorithm. Section 6 gives our conclusions and directions of future work.

2 The linear mixing model

The linear mixing model can be expressed as follows:

$$\mathbf{x} = \sum_{i=1}^{M} a_i \mathbf{s}_i + \mathbf{w} = \mathbf{S}\mathbf{a} + \mathbf{w}, \tag{1}$$

where $\mathbf{x}$ is the d-dimension received pixel spectrum vector, $\mathbf{S}$ is the $d \times M$ matrix whose columns are the d-dimension endmembers $\mathbf{s}_i, i = 1, .., M$, $\mathbf{a}$ is the M-dimension fractional abundance vector, and $\mathbf{w}$ is the d-dimension additive observation noise vector. The linear mixing model is subjected to two constraints on the abundances. First, to be physically meaningfull , all abundances must be non-negative $a_i \geq 0, i = 1, .., M$. Second, to account for the entire composition the abundances must be fully additive $\sum_{i=1}^{M} a_i = 1$.

Often the process of spectral unmixing is performed on transformations of the data intended to reduce the computational burden [9] or to enhance some properties of the data [8]. We do not apply any dimension reduction transformation here. The task of endmember determination is the focus of this paper. In an already classical paper [4], Craig starts with the observation that the scatter plots of remotely sensed data are tear shaped or pyramidal, if two or three spectral bands are considered. The apex lies in the so-called dark point. The endmember detection becomes the search for non-orthogonal planes that enclose the data forming a minimum volume simplex, hence the name of the method.

Besides its computational cost the method requires the prespecification of the number of endmenbers. Another step to the automatic endmember detection is the Conical Analysis method proposed in [8] and applied to target detection. The extreme points in the data after a Principal Component transform are the searched for endmember spectra. The method is geometrically similar to the Craig´s one but does not require costly linear programming. It also requires the prespecification of the desired number of endmembers. Another approach is the modelling by Markov Random Fields and the detection of spatially consistent regions whose spectra will be assumed as endmembers [15]. A quite standard approach to endmember determination is the use of standard libreries of spectra [9]. This approach requires great expertise and a prori knowledge of the data. Finally, there are interactive exploration algorithms that are supported by specific software packages.

Once the endmembers have been determined the last task is the computation of the inversion that gives the fractional abundance and, therefore, the spectral unmixing. The simplest approach is the unconstrained least squared error estimation given by:

$$\widehat{\mathbf{a}} = \left(\mathbf{S}^T\mathbf{S}\right)^{-1}\mathbf{S}^T\mathbf{x}. \tag{2}$$

The abundances that result from this computation do not fulfill the non-negative and full aditivity conditions. It is possible to enforce each condition separately, but rather difficult to enforce both simultaneously [9]. As our aim is to test an endmember determination procedure, therfore we will use unconstrained estimation (2) to compute the abundance images. We will show intensity scaled and shifted images of the abundances to evaluate our results.

3 Morphological Associative Memories

The work on Morphological Associative Memories stems from the consideration of an algebraic lattice structure $(\mathbb{R}, \vee, \wedge, +)$ as the alternative to the algebraic $(\mathbb{R}, +, \cdot)$ framework for the definition of Neural Networks computation [16] [17]. The operators $\vee$ and $\wedge$ denote, respectively, the discrete max and min operators (resp. sup and inf in a continuous setting). The approach is termed morphological neural networks because $\vee$ and $\wedge$ correspond to the morphological dilation and erosion operators, respectively. Given a set of input/output pairs of pattern $(X, Y) = \left\{\left(\mathbf{x}^\xi, \mathbf{y}^\xi\right); \xi = 1, .., k\right\}$, an heteroassociative neural network based on the pattern's crosscorrelation [10], [7] is built up as $W = \sum_\xi \mathbf{y}^\xi \cdot \left(\mathbf{x}^\xi\right)'$. Mimicking this construction procedure [16], [17] propose the following constructions of HMM's:

$$W_{XY} = \bigwedge_{\xi=1}^{k} \left[\mathbf{y}^\xi \times \left(-\mathbf{x}^\xi\right)'\right] \qquad M_{XY} = \bigvee_{\xi=1}^{k} \left[\mathbf{y}^\xi \times \left(-\mathbf{x}^\xi\right)'\right] \tag{3}$$

where $\times$ is any of the $\boxvee$ or $\boxwedge$ operators. Here $\boxvee$ and $\boxwedge$ denote the max and min matrix product, respectively defined as follows:

$$C = A \boxvee B = [c_{ij}] \Leftrightarrow c_{ij} = \bigvee_{k=1..n} \{a_{ik} + b_{kj}\}, \tag{4}$$

$$C = A \boxwedge B = [c_{ij}] \Leftrightarrow c_{ij} = \bigwedge_{k=1..n} \{a_{ik} + b_{kj}\}. \tag{5}$$

It follows that the weight matrices W_{XY} and M_{XY} are lower and upper bounds of the max and min matrix products $\forall \xi; W_{XY} \leq \mathbf{y}^\xi \times \left(-\mathbf{x}^\xi\right)' \leq M_{XY}$ and therefore the following bounds on the output patterns hold $\forall \xi; W_{XY} \boxvee \mathbf{x}^\xi \leq \mathbf{y}^\xi \leq M_{XY} \boxwedge \mathbf{x}^\xi$, that can be rewritten $W_{XY} \boxvee X \leq Y \leq M_{XY} \boxwedge X$. A matrix A is a $\boxvee$-perfect ($\boxwedge$-perfect) memory for (X, Y) if $A \boxvee X = Y$ ($A \boxwedge X = Y$). It can be proven that if A and B are $\boxvee$-perfect and $\boxwedge$-perfect memories, resp., for (X, Y), then W_{XY} and M_{XY} are also $\boxvee$-perfect and $\boxwedge$-perfect, resp.: $A \leq W_{XY} \leq M_{XY} \leq B$. Therefore $W_{XY} \boxvee X = Y = M_{XY} \boxwedge X$. Conditions of perfect recall of the stored patterns are given by the following theorems proved in [16],[17]:

Theorem 1. *Perfect recall of HMM. The matrix W_{XY} is $\boxvee$-perfect if and only if $\forall \xi$ the matrix $\left[\mathbf{y}^\xi \times \left(-\mathbf{x}^\xi\right)' \right] - W_{XY}$ contains a zero at each row. Similarly, the matrix M_{XY} is $\boxwedge$-perfect if and only if $\forall \xi$ the matrix $\left[\mathbf{y}^\xi \times \left(-\mathbf{x}^\xi\right)' \right] - M_{XY}$ contains a zero at each row.*

Theorem 2. *Perfect recall of AMM. Both erosive and dilative AMM's have the perfect recall property: $W_{XX} \boxvee X = X = M_{XX} \boxwedge X$, for any X.*

These results hold when we try to recover the output patterns from the noise-free input pattern. To take into account the noise, a special definition of the kinds of noise affecting the input patterns is needed. Let it be $\widetilde{\mathbf{x}}^\gamma$ a noisy version of $\mathbf{x}^\gamma$. If $\widetilde{\mathbf{x}}^\gamma \leq \mathbf{x}^\gamma$ then $\widetilde{\mathbf{x}}^\gamma$ is an eroded version of $\mathbf{x}^\gamma$, alternatively we say that $\widetilde{\mathbf{x}}^\gamma$ is subjected to erosive noise. If $\widetilde{\mathbf{x}}^\gamma \geq \mathbf{x}^\gamma$ then $\widetilde{\mathbf{x}}^\gamma$ is a dilated version of $\mathbf{x}^\gamma$, alternatively we say that $\widetilde{\mathbf{x}}^\gamma$ is subjected to dilative noise. Morphological memories are very sensitive to these kinds of noise. The conditions of *robust* perfect recall for W_{XY}, i.e. the retrieval of $\mathbf{y}^\gamma$ given a noisy copy $\widetilde{\mathbf{x}}^\gamma$, are given in [16], [17]. The dilative HMM W_{XY} is robust against controlled erosions of the input patterns while the erosive HMM M_{XY} is robust against controlled dilations of the input patterns. At present we are more concerned by the conditions for perfect recall of noisy patterns of AMM:

Corollary 1. *Given patterns X, the equality $W_{XX} \boxvee \widetilde{\mathbf{x}}^\gamma = \mathbf{x}^\gamma$ holds when the noise affecting the pattern is erosive $\widetilde{\mathbf{x}}^\gamma \leq \mathbf{x}^\gamma$ and the following relation holds $\forall i \exists j_i; \widetilde{x}_{j_i}^\gamma = x_{j_i}^\gamma \vee \left(\bigvee_{\xi \neq \gamma} \left(x_i^\gamma - x_i^\xi + x_{j_i}^\xi \right) \right)$. Similarly, the equality $M_{XY} \boxwedge \widetilde{\mathbf{x}}^\gamma = \mathbf{x}^\gamma$ holds when the noise affecting the pattern is dilative $\widetilde{\mathbf{x}}^\gamma \geq \mathbf{x}^\gamma$ and the following relation holds: $\forall i \exists j_i; \widetilde{x}_{j_i}^\gamma = x_{j_i}^\gamma \wedge \left(\bigwedge_{\xi \neq \gamma} \left(x_i^\gamma - x_i^\xi + x_{j_i}^\xi \right) \right)$.*

The AMM will fail in the case of the noise being a mixture of erosive and dilative noise. To obtain general robutness the kernel method has been proposed [16], [18], [22]. In order to characterize kernels and to obtain a constructive definition, the notion of morphological independence and strong morphological independence is introduced in [18], here we distinguish erosive and dilative versions of this definition:

Definition 1. *Morphological independence. Given a set of pattern vectors $X = \left(\mathbf{x}^1, ..., \mathbf{x}^k\right)$, a pattern vector $\mathbf{y}$ is said to be morphologically independent of X in the erosive sense if $\mathbf{yx}^\gamma; \gamma = \{1, .., k\}$, and morphologically independent of X in the dilative sense if $\mathbf{yx}^\gamma; \gamma = \{1, .., k\}$. The set of pattern vectors X is said to be morphologically independent in either sense when all the patterns are morphologically indenpendent of the remaining patterns in the set.*

The strong morphological independence is introduced in [18] to give a construction for minimal kernels with maximal noise robustness. For binary valued vectors, morphological independence and strong morphological independence are equivalent. For the current application we want to use AMM as detectors of the set extreme points, to obtain a rough approximation of the minimal simplex that covers the data points. We need to establish first a simple fact in the following remark:

Remark 1. Given a set of pattern vectors $X = \left(\mathbf{x}^1, ..., \mathbf{x}^k\right)$ and the erosive W_{XX} and dilatative M_{XX} memories constructed from it. Given a test pattern $\mathbf{y} \notin X$, if $\mathbf{y}$ is morphologically independent of X in the erosive sense, then $W_{XX} \boxtimes \mathbf{y} \notin X$. Also, if $\mathbf{y}$ is morphologically independent of X in the dilative sense, then $M_{XX} \boxtimes \mathbf{y} \notin X$.

The endmembers that we are searching for are the corners of a high dimensional box centered at the origin of the space (we will perform a simple correction of the mean of the data). They are morphologically independent vectors both in the erosive and dilative senses, and they enclose the remaining vectors. The endmember detection process would apply the erosive and dilative AMM's constructed from the already detected endmembers to detect the new ones as suggested by the previous remark. Working with integer valued vectors, a desirable property is that vectors already inside the box defined by the endmembers would be detected as such. However, given a set of pattern vectors $X = \left(\mathbf{x}^1, ..., \mathbf{x}^k\right)$ and the erosive W_{XX} and dilatative M_{XX} memories constructed from it. If a test pattern $\mathbf{y} < \mathbf{x}^\gamma$ for some $\gamma \in \{1, .., k\}$ would give $W_{XX} \boxtimes \mathbf{y} \notin X$. Also, if the test pattern $\mathbf{y} > \mathbf{x}^\gamma$ for some $\gamma \in \{1, .., k\}$ then $M_{XX} \boxtimes \mathbf{y} \geq \notin X$. Therefore, working with integer valued patterns the detection of the morphologically independent patterns would be impossible. However, if we consider the binary vectors obtained as the sign of the vector components, then morphological independence would be detected as suggested by the above remark. Let us denote by the expression $\mathbf{x} > \mathbf{0}$ the construction of the binary vector $\left(\{b_i = 1 \text{ if } x_i > 0; b_i = 0 \text{ if } x_i \leq 0\}; i = 1, .., n\right)$.

4 The detection of spectral endmembers

The endmembers of a given hyperespectral image under the linear mixture assumption correspond to the vertices of the minimal simplex that encloses the data points. The region of the space enclosed by a set of vectors simultaneously morphologically independent in both erosive and dilative senses is a high dimensional box. Therefore, the search for the extremes in the morphological sense gives the high dimensional box that best approaches the minimal simplex that encloses the data points. The approach in this paper is to use AMM's as the mechanism to evaluate the morphological independence condition. Let us denote $\left\{ \mathbf{f}\left(i, j\right) \in \mathbb{R}^d; i = 1, .., n; j = 1, .., m \right\}$ the hyperspectral image, $\boldsymbol{\mu}$ and $\boldsymbol{\sigma}$ the vectors of the mean and standard deviations of each band computed over the image, α the noise correction factor and E the set of endmembers discovered. We perform first a correction of the mean of the data, so that it will be centered about the origin, to ease the detection of the directions where the extreme points lye. The standard deviation of the data at each band is taken as an estimation of the additive noise standard deviation. To test the morphological independence we apply the AMM to the pixel spectra after the addition and substraction of $\alpha\boldsymbol{\sigma}$. This procedure is intended to avoid the detection of small fluctuations around the mean as endmember directions. The confidence level α controls the amount of flexibility in the discovering of new endmembers.

The steps in the procedure are the following:

1. Compute the zero mean image $\{\mathbf{f}^c\left(i, j\right) = \mathbf{f}\left(i, j\right) - \boldsymbol{\mu}; i = 1, .., n; j = 1, .., m\}$.
2. Initialize the set of endmembers $E = \{\mathbf{e}_1\}$ with a pixel spectra randomly picked from the image. Initialize the set of morphologically independent binary signatures $X = \{\mathbf{x}_1\} = \left\{\left(e_k^1 > 0; k = 1, .., d\right)\right\}$
3. Construct the AMM's based on the morphologically independent binary signatures: M_{XX} and W_{XX}. Define orthogonal binary codes Y for the endmembers and construct the identification HMM[4]: M_{XY}.
4. For each pixel $\mathbf{f}^c\left(i, j\right)$
   (a) compute the vector of the signs of the Gaussian noise corrections $\mathbf{f}^+\left(i, j\right) = \left(\mathbf{f}^c\left(i, j\right) + \alpha\boldsymbol{\sigma} > \mathbf{0}\right)$ and $\mathbf{f}^-\left(i, j\right) = \left(\mathbf{f}^c\left(i, j\right) - \alpha\boldsymbol{\sigma} > \mathbf{0}\right)$
   (b) compute $y^+ = M_{XY} \boxtimes \left(M_{XX} \boxtimes \mathbf{f}^+\left(i, j\right)\right)$
   (c) compute $y^- = M_{XY} \boxtimes \left(W_{XX} \boxtimes \mathbf{f}^-\left(i, j\right)\right)$
   (d) if $y^+ \notin Y$ and $y^- \notin Y$ then $\mathbf{f}^c\left(i, j\right)$ is a new endmember to be added to E, go to step 3 and resume the exploration of the image.
   (e) if $y^+ \in Y$ and $\mathbf{f}^c\left(i, j\right) > \mathbf{e}_{y^+}$ the pixel spectral signature is more extreme than the stored endmember, then substitute $\mathbf{e}_{y^+}$ with $\mathbf{f}^c\left(i, j\right)$.
   (f) if $y^- \in Y$ and $\mathbf{f}^c\left(i, j\right) < \mathbf{e}_{y^-}$ the pixel is more extreme than the stored endmember, then substitute $\mathbf{e}_{y^-}$ with $\mathbf{f}^c\left(i, j\right)$.
5. The final set of endmembers is the set of original spectral signatures $\mathbf{f}\left(i, j\right)$ of the pixels selected as members of E.

---

[4] Although we have no formal proof of the perfect recall of the HMM when the input patterns are morphologically independent, it is very likely and fits nicely to use the HMM as the endmember identifier. In practice, we search the set X directly.

5 Experimental results

The spectra used for this work correspond to the Indian Pines 1992 image obtained by the Airborne Visible/Infrared Imaging Spectrometer (AVIRIS) developed by NASA JPL which has 224 contiguous spectral channels covering a spectral region form 0.4 to 2.5 mm in 10 nm steps. It is a 145 by 145 pixel image with 220 spectral bands that contains a distribution of two-thirds of agricultural land and one-third of forest and other elements (two highways, a rail line and some houses and smaller roads). The ground truth available for this image [11] designates 16 mutually exclusive classes of land cover. Examples of studies about the application of supervised classification algorithms to this image are [3], [24], [25], [26]. Figure 1 shows the ground truth as identified in [11], [25]. Many specific charateristics are hidden in the background class. The distribution of the cover classes was drawn approximately, so there is a non neglible amount of erronously labeled pixels in the ground truth. The results of the supervised classification show a great deal of details [3], [25]. As we do not have the permission to reproduce these results we present in figure 2 some false color renderings based on different band selections. These images highligh some spatial distributions of land cover that are consistently identified by diverse works on supervised classification.

We have applied our method to the endmember detection starting with different initializations of the endmember set. In all cases the number of detected endmembers was in the range from 8 up to 15. The control parameter α was set at values between 2 and 1.6, the lower the values the greater the number of endmember detected. The image pixels were processed once. As the endmember detection is an unsupervised process, although we have a ground truth we don't have any proper performance measure, unlike the supervised classification case. The validation of the quality of the results must be by observation of the resulting abundance images. In these images white correspond to high values and black to low values (may be negative). We present in figure 4 abundance images resulting from an execution of the algorithm.

For instance, the endmember #1 seems to be a good detector for oats, whose ground truth spatial situation can be appreciated in figure 1. Abundance image 1 highlights the ground truth patch, but also several straight lines that may correspond to borders between land lots and to the side trees of roads. Endmember #5 appears to be specialized in cultivated lands, it highlights the oats but also the other crops, it gives very dark response on the woods while endmember #7 is a good detector of woods and grass, according to the ground truth and the results of supervised classification [25]. If we take into account that the data was gathered when the crops were very low, a feasible interpretation of the results is that endmember #5 is detecting the soil, while endmember #7 detects the green cover of the woods and the grass. This discussion is aimed to show that the endmembers detected may have some physical meaning and some value in the analysis and interpretation of the image.

8
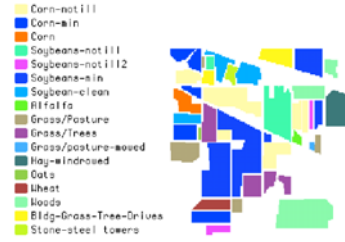
Fig. 1. The Indian Pines image ground truth
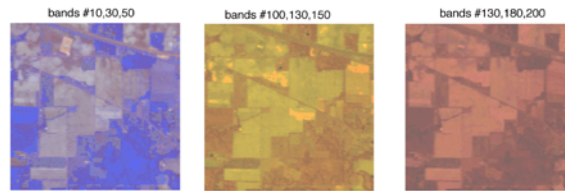
Fig. 2. Some false color renderings of the image based on different selections of the bands that correspond to the RGB.
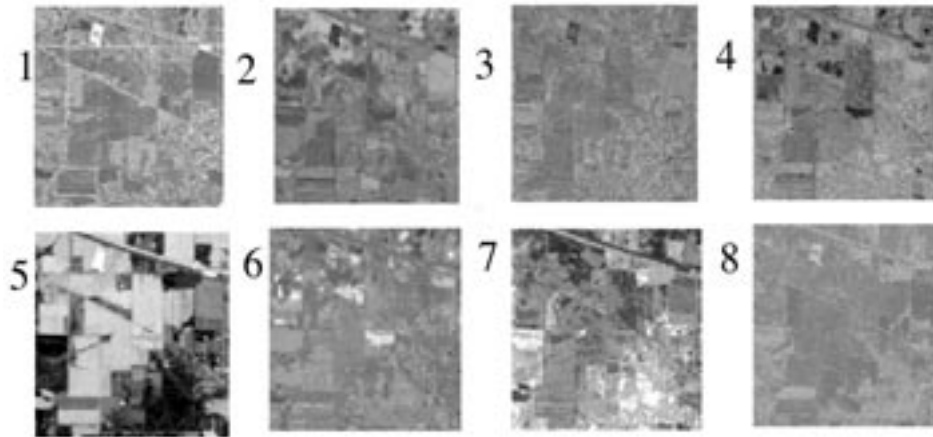
Fig. 3. Abundance images computed using the endmembers in figure 3.

6   Conclusions and Further Work

We have proposed an algorithm for endmember detection in hyperespectral images based on the noise sensitivity of the Autoassociative Morphological Memories (AMM). The procedure does not need the a priori setting of the number of endmembers. Its flexibility in the discovering of endmembers is controlled by the amount of noise correction introduced in the pixel spectral signature. Experimental results on the Indian Pines image have demonstrated that the procedure gives a reasonable number of endmembers with little tuning of the control parameter (α), and that these endmembers have physical meaning and may serve for the analysis of the image.

Further work must be addressed to experimentation with other multi and hyperspectral images to further validate the approach. Also, research into the realization of learning processes on morphological neural networks for this task is a promising research venue. It involves the shift from binary clasification as performed by the min/max networks into morphological category representative detection (clustering).

Acknowledgements

References

1. Asano A., K. Matsumura, K. Itoh, Y. Ichioka, S. Yokozeki, (1995) Optimization of morphological filters by learning, Optics Comm. 112 : 265-270
2. Carpenter G.A., S. Grossberg, D.B. Rosen, (1991) Fuzzy ART: Fast stable learning of analog patterns by an adaptive resonance system, Neural Networks 4:759-771,
3. Crespo J.L., R. Duro, Hyperspectral Image Segmentation through Gaussian Synapse Networks , submitted ICANN'2002
4. Craig M., Minimum volume transformations for remotely sensed data, IEEE Trans. Geos. Rem. Sensing, 32(3):542-552
5. Gader P.D., M.A. Khabou, A. Kodobobsky (2000) Morphological regularization neural networks, Pattern Recognition 33 pp. 935-944
6. Graña M., B. Raducanu. (2001) On the application of morphological heteroassociative neural networks. Proc. Int. Conf. on Image Processing (ICIP), I. Pitas (ed.), pp.501-504, Thessaloniki, Greece, October , IEEE Press.
7. Hopfield J.J., (1982) Neural networks and physical systems with emergent collective computational abilities, Proc. Nat. Acad. Sciences, vol. 79, pp.2554-2558,
8. Ifarraguerri A., C.-I Chang, (1999) Multispectral and Hyperspectral Image Analysis with Convex Cones, IEEE Trans. Geos. Rem. Sensing, 37(2):756-770
9. Keshava N., J.F. Mustard Spectral unimixing, IEEE Signal Proc. Mag. 19(1) pp:44-57 (2002)

10. Kohonen T. , (1972) Correlation Matrix Memory, IEEE Trans. Computers, 21:353-359,

11. Landgrebe D. , Indian Pines AVIRIS Hyperspectral Reflectance Data: 92av3c, 1992. The full data set is called Indian Pines 1 920612B available at http://makalu.jpl.nasa.gov/locator/index.html.

12. Pessoa L.F.C , P. Maragos, (1998) MRL-filters: a general class of nonlinear systems and their optimal design for image processing, IEEE Trans. on Image Processing, 7(7): 966 -978,

13. Pessoa L.F.C , P. Maragos (2000) Neural Networks with hybrid morphological/rank/linear nodes: a unifying framework with applications to handwritten character recognition, Patt. Rec. 33: 945-960

14. Raducanu B. , M. Graña, P. Sussner.(2001) Morphological neural networks for vision based self-localization. Proc. of ICRA2001, Int. Conf. on Robotics and Automation, pp. 2059-2064, Seoul, Korea, May , IEEE Press.

15. Rand R.S., D.M.Keenan (2001) A Spectral Mixture Process Conditioned by Gibbs-Based Partitioning, IEEE Trans. Geos. Rem. Sensing, 39(7):1421-1434

16. Ritter G. X., J. L. Diaz-de-Leon, P. Sussner. (1999) Morphological bidirectional associative memories. Neural Networks, Volume 12, pages 851-867,

17. Ritter G. X., P. Sussner, J. L. Diaz-de-Leon. (1998) Morphological associative memories. IEEE Trans. on Neural Networks, 9(2):281-292,

18. Ritter G.X., G. Urcid, L. Iancu, (2002) Reconstruction of patterns from moisy inputs using morphological associative memories, J. Math. Imag. Vision submitted

19. Ritter G. X., J.N. Wilson, Handbook of Computer Vision Algorithms in Image Algebra, Boca Raton, Fla: CRC Press

20. Rizzi A., M. ,F.M. Frattale Mascioli, (2002) Adaptive resolution Min-Max classifiers, IEEE trans Neural Networks 13 (2):402-414.

21. Salembier P. (1992) Structuring element adaptation for morphological filters, J. Visual Comm. Image Repres. 3: 115-136

22. Sussner P., (2001) Observations on Morphological Associative Memories and the Kernel Method, Proc. IJCNN'2001, Washington DC, July

23. Sussner P. (2002) , Generalizing operations of binary autoassociative morphological memories using fuzzy set theory, J. Math. Imag. Vision submitted

24. Tadjudin, S. and D. Landgrebe, (1998). Classification of High Dimensional Data with Limited Training Samples. PhD Thesis and School of Electrical & Computer Engineering Technical Report TR-ECE 98-8, Purdue University.

25. Tadjudin, S. and D. Landgrebe,(1999) Covariance Estimation with Limited Training Samples, IEEE Trans. Geos. Rem. Sensing, 37(4):2113-2118,

26. Tadjudin, S. and D. Landgrebe, (2000) Robust Parameter Estimation for Mixture Model, IEEE Trans. Geos. Rem. Sensing, 38(1):439-445,

27. Won Y., P. D. Gader, P.C. Coffield, (1997) Morphological shared-weight neural network with applications to automatic target detection, IEEE Trans. Neural Networks, 8(5): 1195 -1203,

28. Yang P.F., P. Maragos, (1995) Min-Max Classifiers: learnability, design and application, Patt. Rec. 28(6):879-899

29. Zhang X.; C. Hang; S. Tan; PZ. Wang, (1996) The min-max function differentiation and training of fuzzy neural networks, IEEE trans. Neural Networks 7(5):1139 -1150,